TROSY NMR for Studies of Large Biological Macromolecules in Solution

César Fernández[1] and Gerhard Wider[2]
[1]*Novartis Institutes for Biomedical Research, CH-4002 Basel, Switzerland; and*
[2]*Institute of Molecular Biology & Biophysics, ETH Zurich, CH-8093 Zurich, Switzerland*

Abstract

Transverse relaxation-optimized spectroscopy (TROSY), in combination with isotope labeling techniques and with improvements in NMR instrumentation, have greatly extended applications of NMR spectroscopy to large biological macromolecules that were otherwise not accessible to high-resolution solution state NMR. Important recent applications of TROSY include the structure determinations of integral membrane proteins in detergent micelles, structural and functional studies of large proteins in monomeric form and in macromolecular complexes, and investigations of intermolecular interactions in large complexes. Moreover, TROSY can improve measurements of NMR parameters, such as residual dipolar couplings and scalar couplings across hydrogen bonds, which contribute to a further improvement of the quality and the precision of solution structures of large proteins and oligonucleotides.

Introduction

During the past two decades, liquid-state NMR studies of biological macromolecules have been limited to relatively small structures with molecular weights in the range of 2–25 kDa, with an average around 10 kDa [1]. For biological macromolecules with molecular weights above 25–30 kDa the quality of the NMR data rapidly deteriorates. A major limitation when working with these large molecules arises from the fast relaxation of the NMR signal, causing severe line broadening, which translates into poor spectral resolution and low signal-to-noise ratios. Considerable efforts are devoted to extend applications of solution NMR to larger molecular systems, which would allow, for instance, structure determinations of proteins that cannot be crystallized, including integral membrane proteins, investigations of intermolecular interactions involving large molecules and macromolecular assemblies, and the structure determination of larger oligonucleotides and their complexes with proteins.

Substantial quality improvement of NMR spectra of biological macromolecules with molecular weights above ~25 kDa can be obtained with deuterium labeling (for reviews, see Refs. [2–5]). With the introduction of transverse relaxation-optimized spectroscopy (TROSY) [6–11], relaxation could be reduced to such an extent that satisfactory NMR spectra can be obtained from particles with molecular weights far above 100 kDa. Along with improved instrumentation, TROSY has greatly extended the size limit for macromolecules that can be studied by solution NMR, opening a wide range of new applications [12–15]. In this chapter, the basis of TROSY and recent applications of TROSY for structural and functional studies of large biological macromolecules will be reviewed.

Technical Background

The NMR Signal

NMR measures the response of nuclear spins in a large, homogenous magnetic field to perturbations caused by the irradiation of electromagnetic fields in the radio-frequency range [16]. In practice, a sequence of radio-frequency pulses is applied, which are separated by interpulse time periods. The response to such a NMR pulse sequence (Figure 1) is a sum of radio-frequencies that have been emitted by the nuclei.

The NMR signal decays exponentially with a characteristic time constant, the transverse relaxation time T_2 (Figure 1A). For the analysis, the signal is Fourier-transformed (FT) into a spectrum containing resonance lines that represent the various emitted radio-frequencies. The width of the resonance lines in the spectrum is inversely proportional to T_2, which depends on the size of the molecule: for increasing molecular masses, T_2 becomes shorter (fast transverse relaxation) and consequently the lines in the spectrum broaden (Figure 1B).

NMR and Molecular Size

When studying large molecules by solution NMR, three major difficulties arise: signal overlap, limited solubility and fast relaxation. In principle, signal overlap can be

Graham A. Webb (ed.), Modern Magnetic Resonance, 483–492.

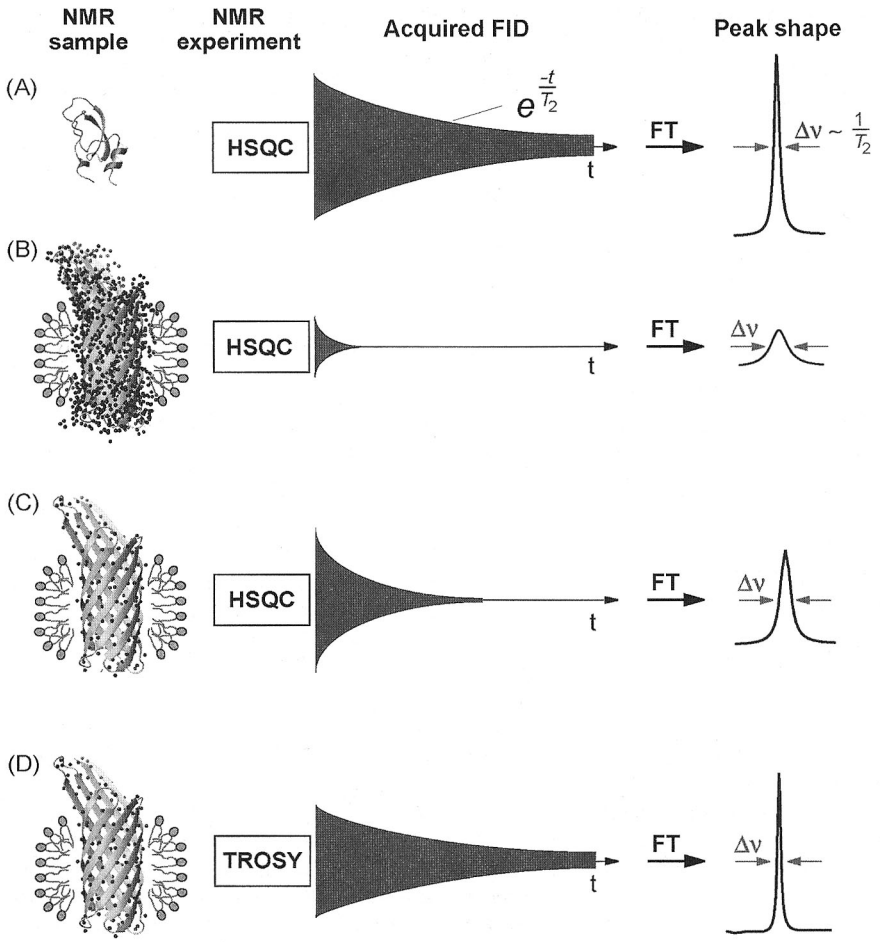

Fig. 1. Solution NMR spectroscopy with small and large molecules. (A) The NMR signal obtained from small molecules in solution relaxes slowly; it has a long transverse relaxation time T_2. Long T_2 values translate into narrow linewidths ($\Delta\nu$) in the NMR spectrum after FT of the NMR signal. HSQC stands for the pulse sequence; the structure on the left hand side represents a small protein. (B) For larger molecules the decay of the NMR signal is faster (T_2 is shorter). This results in a weaker signal after the NMR pulse sequence and broad lines in the spectra. In the schematic structure on the left hand side, the high density of protons is indicated by black dots. (C) By deuteration of the macromolecule (reduced number of protons indicated by less black dots in the schematic structure on the left), the transverse relaxation can be substantially reduced, which yields improved spectral resolution and improved sensitivity for large molecules. (D) Using TROSY pulse sequences with deuterated macromolecular samples the transverse relaxation can be further reduced, thereby increasing considerably the molecular weight amenable to NMR. Adapted from Ref. [14] with permission.

alleviated by proper choice of isotope-labeling schemes, including uniform, segmental, and selective ^{15}N and ^{13}C-labeling techniques [2,17–19]. Limited solubility translates into poor sensitivity, a problem that can be alleviated by new developments in NMR techniques and instrumentation that increase sensitivity, e.g. the development of cryogenic probes and spectrometers with higher magnetic fields.

The limitations caused by nuclear transverse relaxation poses the most severe technical challenge for studies of larger biological macromolecules in solution. Relaxation becomes especially bothering with long and relatively complex pulse sequences that are required for heteronuclear multidimensional NMR experiments. For larger systems, fast transverse relaxation reduces the signal intensities beyond the detection limit before the

desired signal can be measured. The combination of deuteration techniques and TROSY alleviate the deleterious effects of transverse relaxation in such systems and increase the molecular size limit (Figure 1C and D).

Isotope Labeling

A major source for transverse relaxation are the protons in the omnipresent hydrogen atoms. Via dipole–dipole (DD) interactions, they efficiently relax any NMR active nuclei, e.g. ^{1}H, ^{13}C or ^{15}N, in macromolecules. The strength of the DD interaction can be greatly reduced by replacing protons by deuterons, because of the much smaller dipole moment of ^{2}H compared to ^{1}H [2]. Deuteration has clear advantages with regard to relaxation [2–4,20], however, protons contribute a major part of the structural information and produce the most sensitive NMR signal. Thus, measuring completely deuterated proteins is not an option and a compromise has to be found. For example, C–H moieties in macromolecules are often deuterated only to a certain extent, e.g. to 70%, or protons are selectively re-introduced into otherwise highly deuterated molecules, e.g. in methyl groups of Val, Leu, and Ile residues [2,5].

For NMR measurements, biological macromolecules are usually dissolved in H_2O, where their exchangeable ^{15}N–^{1}H groups generally become protonated. The strategically important amide groups in the polypeptide backbone of proteins are thus accessible to ^{1}H NMR experiments. Although deuteration of the C–H groups reduces significantly DD interactions between ^{15}N–^{1}H moieties and remote protons, i.e. the protons outside the ^{15}N–^{1}H group (Figure 1C), the ^{15}N–^{1}H DD interactions are omnipresent in ^{15}N-labeled samples. It has been shown that these ^{15}N–^{1}H DD interactions can be reduced by spectroscopic means using TROSY [6] (Figure 1D).

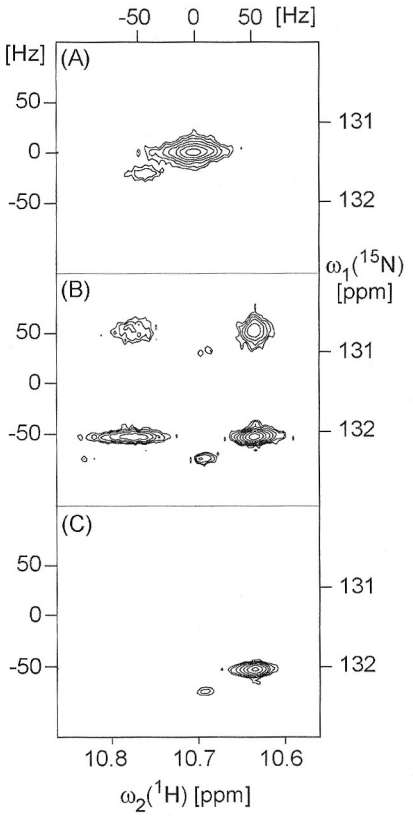

Fig. 2. Contour plots of a backbone amide ^{15}N–^{1}H correlation peak extracted from three different variants of 2D [^{15}N,^{1}H] correlation experiments. (A) Conventional broad-band decoupled [^{15}N,^{1}H]-HSQC. (B) Same as (A) without any decoupling during the experiment. (C) [^{15}N,^{1}H]-TROSY spectrum. Adapted from Ref. [6] with permission.

Transverse Relaxation-Optimized Spectroscopy

The Foundations of TROSY

The TROSY technique [6] is based on the interference of different relaxation mechanisms that contribute to the relaxation of a particular nucleus. This interference can be additive or subtractive resulting in increased or reduced relaxation, respectively. In addition to the omnipresent relaxation due to DD coupling, chemical shift anisotropy (CSA) of ^{1}H, ^{15}N, and ^{13}C can be a significant source of transverse relaxation at the high magnetic fields typically used for studies of biological macromolecules. The interference between this two relaxation mechanisms can be nicely illustrated in a correlation spectrum of ^{15}N and ^{1}H nuclei of amide groups in a polypeptide backbone (Figure 2). Each ^{1}H nucleus couples to its directly attached ^{15}N nucleus via scalar coupling. The ^{1}H NMR spectrum of such an amide moiety thus consists of two lines representing the protons attached to ^{15}N nuclei with spin up and spin down, respectively. The corresponding effect is observed for the ^{15}N nucleus. Therefore, in a 2D correlation experiment without decoupling a four-line fine structure is observed (Figure 2B). In conventional NMR experiments, the four multiplet lines are collapsed into one resonance by decoupling. Decoupling averages the relaxation rates (Figure 2A), which for smaller molecules, where all four multiplet components have almost identical linewidths, results in a simplified spectrum with improved sensitivity. However, for large molecules the multiplet components have largely different linewidths (Figure 2B) and decoupling results in a broad line (Figure 2A) which is much broader and less intense than the narrowest multiplet component (Figure 2C). In this situation it would be an advantage to record only the narrowest component.

The TROSY technique selects exclusively the slowest relaxing component of the four line pattern (Figure 2C) eliminating the faster relaxing multiplet components. Thus, TROSY neglects part of the potential signal, which is, however, more than compensated in large molecules by the much slower relaxation during the pulse sequence and the acquisition (Figure 1D).

Field Strength Dependence of TROSY for $^{15}N-^{1}H$ Groups

The amide proton of a $^{15}N-^{1}H$ moiety relaxes due to DD interaction with the nitrogen and its own CSA. These two interfering relaxation mechanisms lead to different relaxation rates for the two multiplet components of the proton, with one rate smaller and the other one larger than the average rate. This effect depends on the external magnetic field since only CSA relaxation and not DD relaxation is field dependent. The optimal TROSY effect for one doublet component can thus be obtained by choosing the appropriate field strength, where its relaxation rate will be near zero. For amide protons in polypeptides, this "magic field" is about 23.5 T, corresponding to a proton resonance frequency of approximately 1000 MHz. The ^{15}N nucleus in an amide moiety shows a similar interference between $^{15}N-^{1}H$ DD interaction and its CSA, which minimizes the ^{15}N relaxation, accidentally, at about the same "magic field."

In practice, small deviations are expected from the "magic field" calculated for an isolated two-spin system, since the CSA varies slightly depending on the exact geometry of the amide moieties. Further, residual DD couplings (especially of amide protons) with remote protons give rise to relaxation that cannot be compensated by the TROSY effect, but that can be minimized by sample deuteration. In general, one approaches the optimal TROSY effect for peptide $^{15}N-^{1}H$ groups, manifested in optimal resolution and sensitivity, at the highest presently available ^{1}H frequencies of 900 MHz [6] using deuterated samples in aqueous solutions.

Implementation of TROSY: 2D [^{15}N, ^{1}H]-TROSY

The simplest implementation of TROSY into experimental schemes is the 2D [^{15}N,^{1}H]-TROSY [6,21], which does not contain any heteronuclear decoupling, neither during the ^{15}N chemical shift evolution period (t_1), nor during the signal acquisition period (t_2). Without decoupling, the four transitions that correspond to the multiplet components with different relaxation rates (Figure 2) are not mixed. The selection of the slowest relaxing component and the concomitant elimination of the remaining three components are achieved by phase cycling of the rf-pulses. The polarization transfer element ST2-PT [22] retains 50% of the original proton polarization. This residual polarization, however, is slowly relaxing and leads to an overall gain in signal intensity for large biological macromolecules. In general, when working with molecular sizes above 20 kDa at magnetic field strengths corresponding to a proton resonance frequency of at least 700 MHz, a higher signal-to-noise ratio is readily obtained with TROSY when compared with the corresponding conventional experiments.

[$^{13}C-^{1}H$]-TROSY

The application of the TROSY principle is not limited to $^{15}N-^{1}H$ groups in biological macromolecules. $^{13}C-^{1}H$ TROSY can be implemented in experiments with aromatic rings and methyl groups, where cross-correlated relaxation effects are also observed. In aromatic spin systems, the relaxation mechanisms for optimizing ^{1}H and ^{13}C transverse relaxation are $^{13}C-^{1}H$–DD coupling and ^{13}C-CSA [8,23]. The large CSA values for ^{13}C can provide efficient compensation of ^{13}C transverse relaxation by dipolar coupling to the attached proton. In contrast, the small CSA of aromatic protons is not suitable for the application of TROSY and protons are decoupled from ^{13}C during acquisition. For aromatic $^{13}C-^{1}H$ groups the optimal TROSY effect is observed at a ^{1}H frequency of 600 MHz. For ^{13}C-labeled biological macromolecules of any molecular weight, significant sensitivity enhancement in $^{13}C-^{1}H$ correlation spectra of aromatic spin systems can be obtained with the use of TROSY compared to the conventional HSQC-based experiments.

A $^{13}C-^{1}H$ TROSY effect can also be observed in methyl groups, where different dipolar interactions compensate each other in large molecules. In methyl groups, the dominant relaxation of a methyl ^{13}C-nucleus originates in the dipolar coupling with the three methyl protons [24]. Interestingly, the standard [^{13}C,^{1}H]-HMQC correlation experiment is an optimized TROSY experiment for methyl carbons, which maintains 50% of the carbon magnetization in slowly relaxing states. For large molecules the 2D [^{13}C,^{1}H]-HMQC experiment yields superior resolution and sensitivity compared to the [^{13}C,^{1}H]-HSQC experiment, which mixes fast and slowly relaxing transitions, deteriorating significantly the spectral quality. It is important to note that the dipolar interaction is field independent and, therefore, the methyl TROSY can be applied at all field strengths for large molecules [25].

TROSY Applications for Studies of Large Biological Macromolecules

Although collection of high-quality data for structure determination of proteins with molecular masses up to ~100 kDa is now technically feasible, the complexity of the NMR spectra generally increases with the size of the molecule studied and the concomitant signal overlap may limit spectral analysis. Therefore, the preferred

current use of relaxation-optimized NMR techniques is with large structures that yield relatively simple spectra compared to monomeric globular proteins of the same molecular size, such as homo-oligomeric proteins, individual small or medium-size subunits in large molecular complexes and membrane proteins in detergent micelles [12,14].

2D [^{15}N,^{1}H] TROSY

For large proteins, 2D [^{15}N,^{1}H]-TROSY provides fingerprints with improved resolution and sensitivity compared to conventional experiments (Figure 3A). This extends applications based on 2D [^{15}N,^{1}H] correlation experiments to much larger structures, e.g. for studies of intermolecular interactions, either with low-molecular weight ligands or with other biological macromolecules, which are usually applied in NMR screening to detect binding of compounds that can be optimized to high-affinity ligands by "SAR-by-NMR" [26].

TROSY-based NMR experiments have been applied to a variety of macromolecular complexes. They include the 51-kDa complex formed between the pilus chaperone FimC and the pilus subunit FimH from *Escherichia coli* [27], the P-domain of the lectin chaperone calreticulin and Erp57 in a 66.5-kDa complex [28], the p53 core domain bound in a ~200-kDa complex with Hsp90 [29], a 64-kDa immunoglobulin complex with a domain of protein A [30], and the 91-kDa 11-mer TRAP protein [31]. Recently, application of TROSY to malate synthase G from *E. coli*, an 81-kDa monomeric enzyme, yielded valuable quantitative information on ligand binding based on chemical shift mapping, residual dipolar couplings (RDCs), amide proton exchange rates, and ^{15}N spin relaxation measurements [32].

[^{13}C,^{1}H] Correlation Experiments

The simplest experiment that exploits the ^{13}C–^{1}H TROSY effect in aromatic systems is the 2D constant-time-[^{13}C–^{1}H]-TROSY [23]. With the application of TROSY, 4- to 10-fold signal enhancement has been achieved for resonances of the aromatic rings in an 18 kDa protein [23] and for RNA and DNA molecules [33,34]. Based on the [^{13}C,^{1}H]-TROSY building block, 3D pulse sequences can be developed that allow assignments of aromatic spin systems in proteins and nucleic acids [23].

TROSY can also be very profitably applied to methyl groups [35]. With a 2D [^{13}C,^{1}H]-HMQC experiment, sensitivity gains up to a factor of 3 compared to a [^{13}C,^{1}H]-HSQC have been observed for a perdeuterated, selectively methyl-^{1}H,^{13}C-labeled protein with a rotational correlation time of 400–450 ns (equivalent to a ~800 kDa globular molecule at 37 °C) [24,25]. For very large molecules the methyl ^{13}C–^{1}H TROSY effect can be exploited in 2D and 3D experiments for resonance assignments of methyl groups [36], for stereospecific assignments of prochiral methyls [37], for studies of domain orientation based on RDCs and ligand binding [32] and for studies of dynamic properties [38].

TROSY for Resonance Assignments in Large Molecules

^{15}N–^{1}H TROSY for Assignment of Protein Backbone Resonances

Triple-resonance experiments [39–42], which are usually applied for backbone resonance assignments of ^{13}C,^{15}N-labeled proteins, include the amide moiety. These experiments contain extended time periods with transverse amide nitrogen magnetization and yield dramatic signal enhancement when using TROSY. TROSY versions of the most relevant triple resonance experiments have been implemented [43–48], which in general yield sensitivity gains of more than one order of magnitude with proteins in the molecular weight range from 25 to 150 kDa [43–46,49]. As an example, Figure 3 shows the dramatic improvement in spectral quality that can be obtained with TROSY in a molecular complex of about 60 kDa. Whereas the TROSY version shows clear cross peaks (Figure 3C), the conventional spectrum cannot at all yield the desired correlations (Figure 3D).

Using TROSY techniques, resonance assignments have been obtained for much larger proteins than ever thought possible with conventional NMR techniques. This was first demonstrated with a homo-octameric 110 kDa protein [49], where 20- to 50-fold sensitivity gains in triple resonance experiments were observed. More recently, backbone resonance assignments in the 723-residue monomeric protein malate synthase were obtained, which is the largest single polypeptide chain that has been assigned to date [50].

^{15}N–^{1}H TROSY for Assignment of Protein Side-Chain Resonances

In addition to resonance assignments of nuclei in the polypeptide backbone, ^{15}N–^{1}H TROSY experiments have been developed for assignment of ^{1}H and ^{13}C chemical shifts of methyl groups in selectively methyl-protonated and otherwise deuterated large proteins. In one application, the membrane protein OmpX in 60 kDa DHPC micelles [51] has been selectively protonated at the Val, Leu, and Ile (δ1) methyl groups [52]. With ^{15}N–^{1}H TROSY-based ^{13}C–^{13}C TOCSY experiments, the methyl groups were correlated with the backbone amide groups, yielding complete sequence-specific assignments of the protonated methyl groups [51], which had a significant impact

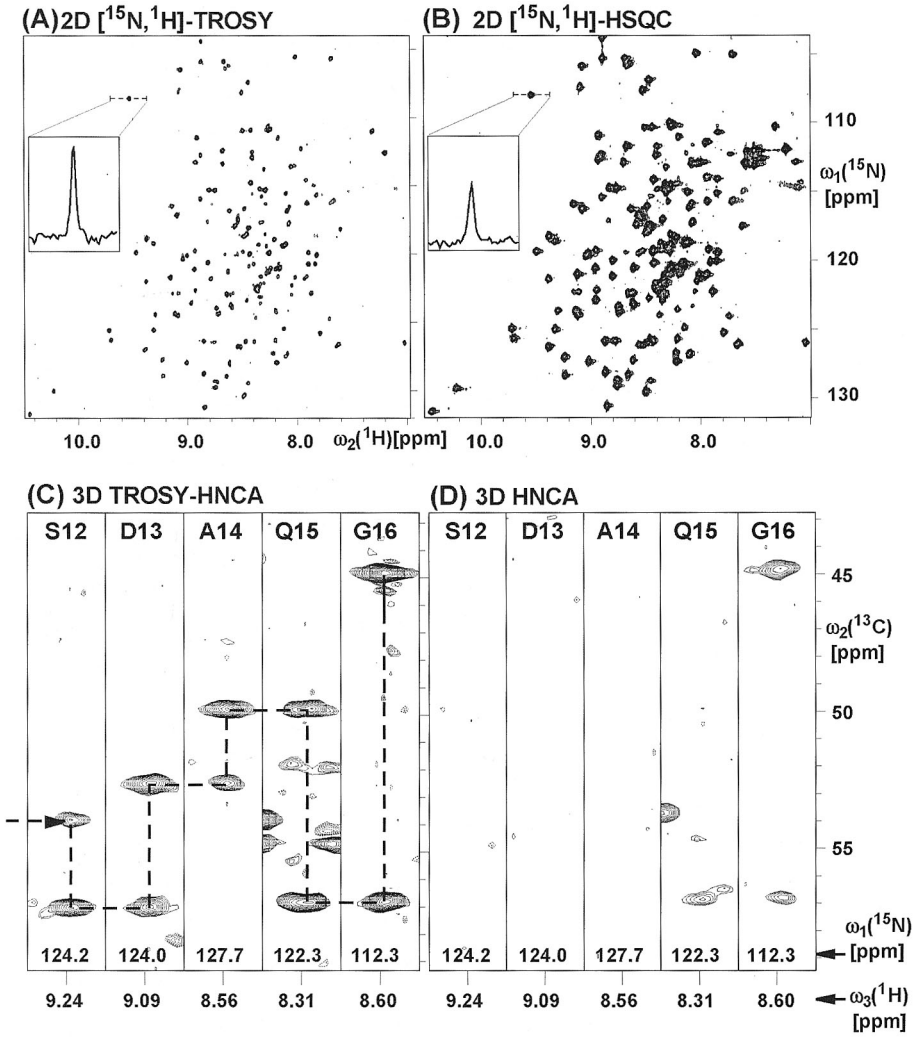

Fig. 3. Impact of TROSY on NMR spectra. The spectra were measured at a ^{1}H resonance frequency of 750 MHz with a sample of the uniformly $^{2}H,^{13}C,^{15}N$-labeled integral membrane protein OmpX in dihexanoylphosphatidylcholine (DHPC) micelles, a 60-kDa complex. (A) and (B) show ^{15}N–^{1}H correlation spectra that were identically recorded and processed, except that TROSY was used in (A) only. The inserts show cross sections that were taken parallel to the ω_2 (^{1}H) axis at the position indicated by the horizontal broken lines. (C) Strips along the ^{13}C-dimension from a 3D [$^{15}N,^{1}H$]-TROSY-HNCA spectrum. The strips were taken at the ^{15}N chemical shifts (indicated at the bottom of the strips) of the amino acid residues 12–16, and are centered at the corresponding amide proton chemical shifts, $\omega_3(^{1}H^{N})$. Horizontal and vertical broken lines indicate the connectivities that can be obtained, leading to complete resonance assignments of the polypeptide backbone $^{1}H^{N}$, ^{15}N, and $^{13}C^{\alpha}$ nuclei. (D) Strips from a conventional 3D HNCA spectrum; the strips were taken at the same frequencies as in (C). Adapted from Ref. [14] with permission.

on the precision of the NMR structure [53]. Recently, near complete assignments of Val, Leu, and Ile ($\delta 1$) methyl groups have been obtained for the 81 kDa protein malate synthase G using new labeling strategies in concert with new TROSY-type NMR experiments [25,36,37]. The Val and Leu isopropyl groups were labeled with ^{1}H and ^{13}C in only one of the two methyl groups, and subsequently assigned using TROSY experiments.

TROSY for Observation of Scalar Couplings Across Hydrogen Bonds

Hydrogen bonds are usually indirectly inferred from experimental data, e.g. from nuclear Overhauser enhancement (NOEs) and proton exchange rates, or from analysis of refined 3D structures based on geometrical considerations. Direct detection of hydrogen bonds in proteins and oligonucleotides was enabled by the observation of scalar spin–spin couplings across hydrogen bonds [54–56]. These couplings allow the determination of hydrogen bond partners, which can be used to refine NMR structures, to study intermolecular interactions at atomic level, and to investigate biological mechanisms involving hydrogen bonding interactions.

The sensitivity and spectral resolution in NMR experiments used to detect hydrogen bonds can be substantially improved for large molecules by using TROSY. Applications include: measurements of scalar couplings across hydrogen bonds in a $^{15}N,^{13}C$-labeled DNA duplex tetradecamer in a 17 kDa protein–DNA complex [55,57], in 25 kDa RNA oligonucleotides [58], in the 30 kDa ribosome-inactivating protein MAP30 [59], in the 147-residue flavoprotein riboflavin 5′-monophosphate [60], and in the active site of the 44 kDa enzyme chorismate mutase [61].

TROSY for Measurements of RDCs

Residual dipolar couplings (RDCs) provide important structural restraints for obtaining global folds and for refining the 3D structure of proteins and oligonucleotides [62–64]. This is especially important in large, perdeuterated molecules, where only a limited number of constraints can be obtained from NOEs [65,66]. Various TROSY-based experimental schemes have been developed for measuring RDCs (for an overview, see Ref. [63]). Applications to the maltose binding protein in a complex with β-cyclodextrin and to carbonic anhydrase II showed that precise RDCs can be obtained for proteins of 30–40 kDa molecular weight [67]. Furthermore, RDCs in the 723-residue malate synthase G [32], in a 53-kDa homomultimeric trimer from mannose binding protein [68], and in the 41-kDa maltose binding protein [69] were measured using TROSY-based experiments.

TROSY for Studies of Dynamic Processes

In addition to structural data, NMR is able to provide information on dynamic processes at atomic resolution over a wide range of time scales [70,71] which can help in understanding structure and function relationships (see, e.g. [72,73]). Key experiments for dynamic studies measure T_1 and T_2 relaxation times, and heteronuclear $^{15}N\{^1H\}$-NOEs of the ^{15}N nuclei in amide groups. For these important experiments, pulse sequences using ^{15}N–^1H TROSY were developed [74,75]. Recently, a new experiment based on methyl TROSY has been applied with the 82 kDa enzyme malate synthase G for studies of slow (millisecond) dynamic processes [38].

TROSY in Nuclear Overhauser Enhancement Spectroscopy

Both, the ^{13}C–^1H and ^{15}N–^1H TROSY effects have been exploited in 3D ^{13}C-resolved and ^{15}N-resolved $[^1H,^1H]$-NOESY experiments, respectively [33,76]. In the pulse sequences of these experiments, TROSY-type chemical shift correlation schemes were used instead of the conventional HSQC or HMQC building blocks. A fully relaxation-optimized ^{15}N-resolved $[^1H,^1H]$-NOESY, the 3D NOESY-$[^1H,^{15}N,^1H]$-zero quantum-TROSY experiment [77], was developed based on TROSY in the ^{15}N–^1H zero quantum state. As an advantage, the usually very intense diagonal peaks are almost completely suppressed in this experiment and weak resonances close to the diagonal become amenable for analysis, alleviating a limitation of conventional NOE spectroscopy. The utility of this approach was demonstrated for the 110 kDa protein aldolase [77].

Applications to Nucleic Acids

For NMR structural studies of nucleic acids, TROSY offers considerable benefits (for a review, see Ref. [78]). Direct detection of hydrogen bonds and measurements of RDCs, which were discussed in the previous sections, are of considerable importance for the structure determination of nucleic acids, since in comparison to proteins, inherently fewer protons are available as sources for structural information. In addition, TROSY has been widely applied to increase the sensitivity and the resolution in correlation experiments for nucleic acids, increasing the range of their applicability to much larger oligonucleotides. Examples include the use of TROSY in correlation experiments [33], in NOESY experiments for the bases [79], in experiments for intra-base and sugar-to-base correlations [34,80,81], and in an experiment that provides correlations between all carbon nuclei in the adenine base [82].

Solution NMR Studies of Membrane Proteins

Membrane proteins take part in important physiological functions, and constitute key targets for drug discovery. Structural studies of membrane proteins by X-ray crystallography or by NMR spectroscopy are much more difficult than for soluble proteins. Since real membrane systems

are far too large for investigation by solution NMR, membrane proteins are often reconstituted in detergent micelles. From these micellar systems, high-quality spectra can be obtained using TROSY (Figure 3) [83–85].

With the availability of TROSY, the first NMR structures of integral membrane proteins in micelles with molecular weights above 50 kDa have been determined, particularly of *E. coli* outer membrane proteins with β-barrel architecture [53,84–88]. The fold of the outer membrane protein OmpX (148 residues) was obtained in DHPC micelles of about 60 kDa molecular mass [53,84,86], the polypeptide backbone fold of the outer membrane protein OmpA (177 residues) has been determined in dodecylphosphocholine (DPC) micelles of 50 kDa molecular mass [87,89], and the backbone fold of the outer membrane enzyme PagP (164 residues) has been determined both in DPC and *n*-octyl-β-D-glucoside micelles of size 50–60 kDa [88,90].

With regard to future developments, recent results obtained for the 39 kDa homotrimeric protein diacylglycerol kinase in micellar complexes with overall sizes larger than 100 kDa [91–93] suggest that NMR-based structure determination of membrane proteins with α-helical architecture, as large and complex as some members of the G-protein-coupled receptor family, may be feasible. Recently, partial backbone resonance assignments have been reported for native bacteriorhodopsin in dodecylmaltoside micelles [94].

Cross-Correlated Relaxation-Induced Polarization Transfer for Studies of Very Large Structures

In heteronuclear NMR experiments, magnetization between the different nuclei is usually transferred based on their scalar spin–spin couplings using INEPT polarization transfer elements [95,96]. During INEPT transfers, TROSY is not active since the slowly and fast relaxing transitions are mixed. For very large structures with molecular weights above approximately 150 kDa, rapid transverse relaxation during the INEPT periods leads to a complete loss of most signals. This limitation can be alleviated by cross-correlated relaxation-enhanced polarization transfer (CRINEPT) [97,98]. In this technique, INEPT and cross-correlated relaxation-induced polarization transfer (CRIPT) [99] are combined. In contrast to INEPT, the transfer efficiency of CRIPT increases proportional to the size of the molecule, so that it becomes an efficient magnetization transfer mechanism for molecules with sizes above 200 kDa [97,98]. Therefore, when studying very large structures significant gains in sensitivity can be achieved by substituting INEPT by CRINEPT or CRIPT.

Methods that allow resonance assignments of macromolecules with molecular weight above ~150 kDa are currently not available and therefore CRINEPT/CRIPT spectroscopy is usually applied to obtain ^{15}N–^{1}H fingerprints of very large structures. As with TROSY-based experiments, the preferred current use of CRINEPT is to study relatively short polypeptide chains (up to ~100–200 amino acid residues) in large supramolecular assemblies, in complexes with large macromolecules, or in large detergent/lipid micelles. The potential of the CRINEPT and CRIPT experiments has recently been demonstrated for 900 kDa complexes formed by GroES with GroEL [98,100].

Conclusion and Outlook

With the development of TROSY, CRINEPT, CRIPT, and isotope labeling techniques, combined with recent advances in NMR instrumentation, solution NMR studies of biological macromolecules with molecular masses well beyond 100 kDa have become a reality. This has been demonstrated in numerous studies dealing with fundamental biological problems, extending from structural investigation of large proteins and the structure determination of the first larger integral membrane proteins in solution, to applications for intermolecular interactions involving relatively large structures [14,15,83,100,101]. The ability to obtain resonance assignments of large biological macromolecules provides the basis for the determination of much larger 3D structures by NMR as thought to be possible just a few years ago. Even if the NMR structure determination is not feasible, the resonance assignment alone can be sufficient to carry out detailed studies of intermolecular interactions and investigations of dynamic processes, which may provide important information on exciting biological systems. However, for very large structures, where CRINEPT and CRIPT are the only means to obtain useful NMR spectra, techniques for resonance assignments are still missing. Nevertheless, NMR fingerprints of proteins with molecular weights up to 900 kDa have been obtained and interesting information could be derived based on the available crystal structure [100].

With the appropriate technical tools available, we expect that many new NMR structures of proteins and nucleic acids with molecular weights above 25 kDa will be elucidated. In this context, techniques that facilitate selective isotope labeling, such as cell-free protein expression [102–105] and segmental isotope labeling [18,19,106,107] may become widely applied to solve larger structures. With the prospect of further advances in NMR techniques and instrumentation, and improved protein expression techniques, larger membrane proteins, as G-protein coupled receptors, may become amenable to solution NMR studies. We are looking forward to future

applications of the techniques described in this review and to technical advances that allow studying even more challenging biological systems.

Acknowledgments

The Novartis Institutes for Biomedical Research (C.F.) and the Schweizerischer Nationalfonds (project 3100A0-100399) (G.W.) are gratefully acknowledged for continuous financial support.

References

1. Güntert P. Q. Rev. Biophys. 1998;31:145 (1998).
2. Gardner KH, Kay LE. Annu. Rev. Biophys. Biomol. Struct. 1998;27:357.
3. LeMaster DM. Prog. NMR Spectrosc. 1994;26:371.
4. LeMaster DM. Q. Rev. Biophys. 1990;23:133.
5. Goto NK, Kay LE. Curr. Opin. Struct. Biol. 2000;10:585.
6. Pervushin K, Riek R, Wider G, Wüthrich K. Proc. Natl. Acad. Sci. U.S.A. 1997;94,:2366.
7. Wider G, Wüthrich K. Curr. Opin. Struct. Biol. 1999;9:594.
8. Pervushin K. Q. Rev. Biophys. 2000;33:161.
9. Riek R, Pervushin K, Wüthrich K. Trends Biochem. Sci. 2000;25:462.
10. Riek R. Meth. Princ. Med. Chem. 2003;16:227.
11. Pervushin K. Biol. Magn. Reson. 2003;20:3.
12. Wüthrich K. Nat. Struct. Biol. 1998;5:492.
13. Venters RA, Thompson R, Cavanagh J. J. Mol. Struct. 2002;602:275.
14. Fernández C, Wider G. Curr. Opin. Struct. Biol. 2003;13:570.
15. Tugarinov V, Hwang PM, Kay LE. Annu. Rev. Biochem. 2004;73:107.
16. Wider G. Prog. NMR Spectrosc. 1998;32:193.
17. Kainosho M. Nat. Struct. Biol. 1997;4(Suppl):858.
18. Yamazaki T, *et al.* J. Am. Chem. Soc. 1998;120:5591.
19. Cowburn D, Muir TW. Methods Enzymol. 2001;339:41.
20. Kushlan DM, LeMaster DM. J. Biomol. NMR. 1993;3:701.
21. Salzmann M, Wider G, Pervushin K, Wüthrich K. J. Biomol. NMR. 1999;15:181.
22. Pervushin K, Wider G, Wüthrich K. J. Biomol. NMR. 1998;12:345.
23. Pervushin K, Riek R, Wider G, Wüthrich K. J. Am. Chem. Soc. 1998;120:6394.
24. Tugarinov V, Hwang PM, Ollerenshaw JE, Kay LE. J. Am. Chem. Soc. 2003;125:10420.
25. Tugarinov V, Kay LE. J. Biomol. NMR. 2004;28:165.
26. Shuker SB, Hajduk PJ, Meadows RP, Fesik SW. Science. 1996;274:1531.
27. Pellecchia M, Sebbel P, Hermanns U, Wüthrich K, Glockshuber R. Nat. Struct. Biol. 1999;6:336.
28. Frickel EM, *et al.* Proc. Natl. Acad. Sci. U.S.A. 2002;99:1954.
29. Rudiger S, Freund SMV, Veprintsev DB, Fersht AR. Proc. Natl. Acad. Sci. U.S.A. 2002;99:11085.
30. Takahashi H, Nakanishi T, Kami K, Arata Y, Shimada I. Nat. Struct. Biol. 2000;7:220.
31. McElroy C, Manfredo A, Wendt A, Gollnick P, Foster M. J. Mol. Biol. 2002;323:463.
32. Tugarinov V, Kay LE. J. Mol. Biol. 2003;327:1121.
33. Brutscher B, Boisbouvier J, Pardi A, Marion D, Simorre JP. J. Am. Chem. Soc. 1998;120:11845.
34. Brutscher B, Simorre JP. J. Biomol. NMR. 2001;21:367.
35. Kreishman-Deitrick M, *et al.* Biochemistry. 2003;42:8579.
36. Tugarinov V, Kay LE. J. Am. Chem. Soc. 2003;125:13868.
37. Tugarinov V, Kay LE. J. Am. Chem. Soc. 2004;126:9827.
38. Korzhnev DM, Kloiber K, Kanelis V, Tugarinov V, Kay LE. J. Am. Chem. Soc. 2004;126:3964.
39. Ikura M, Kay LE, Bax A. Biochemistry. 1990;29:4659.
40. Bax A, Grzesiek S. Acc. Chem. Res. 1993;26:131.
41. Yamazaki T, Lee W, Arrowsmith CH, Muhandiram DR, Kay LE. J. Am. Chem. Soc. 1994;116:11655.
42. Sattler M, Schleucher J, Griesinger C. Prog. NMR Spectrosc. 1999;34:93.
43. Salzmann M, Pervushin K, Wider G, Senn H, Wüthrich K. Proc. Natl. Acad. Sci. U.S.A. 1998;95:13585.
44. Salzmann M, Wider G, Pervushin K, Senn H, Wüthrich K. J. Am. Chem. Soc. 1999;121:844.
45. Yang DW, Kay LE. J. Am. Chem. Soc. 1999;121:2571.
46. Konrat R, Yang DW, Kay LE. J. Biomol. NMR. 1999;15:309.
47. Salzmann M, Pervushin K, Wider G, Senn H, Wüthrich K. J. Biomol. NMR. 1999;14:85.
48. Loria JP, Rance M, Palmer AG. J. Magn. Reson. 1999;141:180.
49. Salzmann M, Pervushin K, Wider G, Senn H, Wüthrich K. J. Am. Chem. Soc. 2000;122:7543.
50. Tugarinov V, Muhandiram R, Ayed A, Kay LE. J. Am. Chem. Soc. 2002;124:10025.
51. Hilty C, Fernández C, Wider G, Wüthrich K. J. Biomol. NMR. 2002;23:289.
52. Goto NK, Gardner KH, Mueller GA, Willis RC, Kay LE. J. Biomol. NMR. 1999;13:369.
53. Fernández C, Hilty C, Wider G, Güntert P, Wüthrich K. J. Mol. Biol. 2004;336:1211.
54. Dingley AJ, Grzesiek S. J. Am. Chem. Soc. 1998;120:8293.
55. Pervushin K, *et al.* Proc. Natl. Acad. Sci. U.S.A. 1998;95:14147.
56. Cordier F, Grzesiek S. J. Am. Chem. Soc. 1999;121:1601.
57. Pervushin K, *et al.* J. Biomol. NMR. 2000;16:39.
58. Yan XZ, Kong XM, Xia YL, Sze KH, Zhu G. J. Magn. Reson. 2000;147:357.
59. Wang YX, *et al.* J. Biomol. NMR. 1999;14:181.
60. Löhr F, Mayhew SG, Ruterjans H. J. Am. Chem. Soc. 2000;122:9289.
61. Eletsky A, *et al.* J. Biomol. NMR. 2002;24:31.
62. Prestegard JH, Al-Hashimi HM, Tolman JR. Q. Rev. Biophys. 2000;33:371.
63. Prestegard JH, Bougault CM, Kishore AI. Chem. Rev. 2004;104:3519.
64. Lipsitz RS, Tjandra N. Annu. Rev. Biophys. Biomol. Struct. 2004;33:387.
65. Mueller GA, *et al.* J. Mol. Biol. 2000;300:197.
66. Choy WY, Tollinger M, Mueller GA, Kay LE. J. Biomol. NMR. 2001;21:31.
67. Yang DW, Venters RA, Mueller GA, Choy WY, Kay LE. J. Biomol. NMR. 1999;14:333.

68. Jain NU, Noble S, Prestegard JH. J. Mol. Biol. 2003;328:451.
69. Evenäs J, Mittermaier A, Yang DW, Kay LE. J. Am. Chem. Soc. 2001;123:2858.
70. Kay LE, Torchia DA, Bax A. Biochemistry. 1989;28:8972.
71. Palmer, AG III. Chem. Rev. 2004;104:3623.
72. Mulder FA, Mittermaier A, Hon A, Dahlquist FW, Kay LE. Nat. Struct. Biol. 2001;8:932.
73. Eisenmesser EZ, Bosco DA, Akke M, Kern D. Science. 2002;295:1520.
74. Zhu G, Xia YL, Nicholson LK, Sze KH. J. Magn. Reson. 2000;143:423.
75. Xia YL, Sze KH,Li N, Shaw PC, Zhu G. Spectrosc.-Int. J. 2002;16:1.
76. Zhu G, Kong XM, Sze KH. J. Biomol. NMR. 1999;13:77.
77. Pervushin K, Wider G, Riek R, Wüthrich K. Proc. Natl. Acad. Sci. U.S.A. 1999;96:9607.
78. Mollova ET, Pardi A. Curr. Opin. Struct. Biol. 2000;10:298.
79. Brutscher B, *et al.* J. Biomol. NMR. 2001;19:141.
80. Riek R, Pervushin K, Fernández C, Kainosho M, Wüthrich K. J. Am. Chem. Soc. 2001;123:658.
81. Fiala R, Czernek J, Sklenar V. J. Biomol. NMR. 2000;16:291.
82. Simon B, Zanier K, Sattler M. J. Biomol. NMR. 2001;20:173.
83. Fernández C, Wüthrich K. FEBS Lett. 2003;555:144.
84. Fernández C, *et al.* FEBS Lett. 2001;504:173.
85. Arora A, Tamm LK. Curr. Opin. Struct. Biol. 2001;11:540.
86. Fernández C, Adeishvili K, Wüthrich K. Proc. Natl. Acad. Sci. U.S.A. 2001;98:2358.
87. Arora A, Abildgaard F, Bushweller JH, Tamm LK. Nat. Struct. Biol. 2001;8:334.
88. Hwang PM, *et al.* Proc. Natl. Acad. Sci. U.S.A. 2002;99:13560.
89. Tamm LK, Abildgaard F, Arora A, Blad H, Bushweller JH. FEBS Lett. 2003;555:139.
90. Hwang PM, Bishop RE, Kay LE. Proc. Natl. Acad. Sci. U.S.A. 2004;101:9618.
91. Oxenoid K, Kim HJ, Jacob J, Sonnichsen FD, Sanders CR. J. Am. Chem. Soc. 2004;126:5048.
92. Oxenoid K, Sönnichsen FD, Sanders CR. Biochemistry. 2002;41:12876.
93. Sanders CR, Sonnichsen FD, Oxenoid K. Paper presented at the Proceedings of the XXth International Conference on Magnetic Resonance in Biological Systems, Toronto, 2002.
94. Schubert M, Kolbe M, Kessler B, Oesterhelt D, Schmieder P. Chembiochem. 2002;3:1019.
95. Morris GA, Freeman R. J. Am. Chem. Soc. 1979;101:760.
96. Burum DP, Ernst RR. J. Magn. Reson. 1980;39:163.
97. Riek R, Wider G, Pervushin K, Wüthrich K. Proc. Natl. Acad. Sci. U.S.A. 1999;96;4918.
98. Riek R, Fiaux J, Bertelsen EB, Horwich AL, Wüthrich K. J. Am. Chem. Soc. 2002;124:12144.
99. Dalvit C. J. Magn. Reson. 1992;97:645.
100. Fiaux J, Bertelsen EB, Horwich AL, Wüthrich K. Nature. 2002;418:207.
101. Wüthrich K, Wider G. Magn. Reson. Chem. 2003;41:S80.
102. Yabuki T, *et al.* J. Biomol. NMR. 1998;11:295.
103. Kigawa T, *et al.* FEBS Lett. 1999;442:15.
104. Kiga D, *et al.* Proc. Natl. Acad. Sci. U.S.A. 2002;99:9715.
105. Yokoyama S. Curr. Opin. Chem. Biol. 2003;7:39.
106. Otomo T, Teruya K, Uegaki K, Yamazaki T, Kyogoku Y. J. Biomol. NMR. 1999;14:105.
107. Cowburn D, Shekhtman A, Xu R, Ottesen JJ, Muir TW. Methods Mol. Biol. 2004;278:47.